

# Aerosol Extinction Uncertainty Determination for a Laser-Based Detecting System

Aimé Lay-Ekuakille and Amerigo Trotta

*Dipartimento d'Ingegneria dell'Innovazione, Università di Lecce,  
Via Arnesano, 73100 Lecce Italy*

**Abstract** Quantitative evaluation of lidar signal is a matter of some complexity. However, it should be noted that, in both qualitative displays and quantitative evaluations, the limiting factor to signal detectability (given adequate sensitivity of the detection and display devices) is the level of noise due to various extraneous sources of signal power. These include thermal noise of the electrical circuits involved, shot and other noise of the photo-detector and, probably most importantly, noise caused by optical energy, normally of solar origin, present as background light, particularly of course, in daytime. This paper presents an alternative way for determining the uncertainty in lidar data with respect to poissonian approach, by implementing a filtering system and a noise modeling with good results.

**Keywords:** Poissonian approach, Filtering, Uncertainties, Noise modeling.

## 1. Introduction

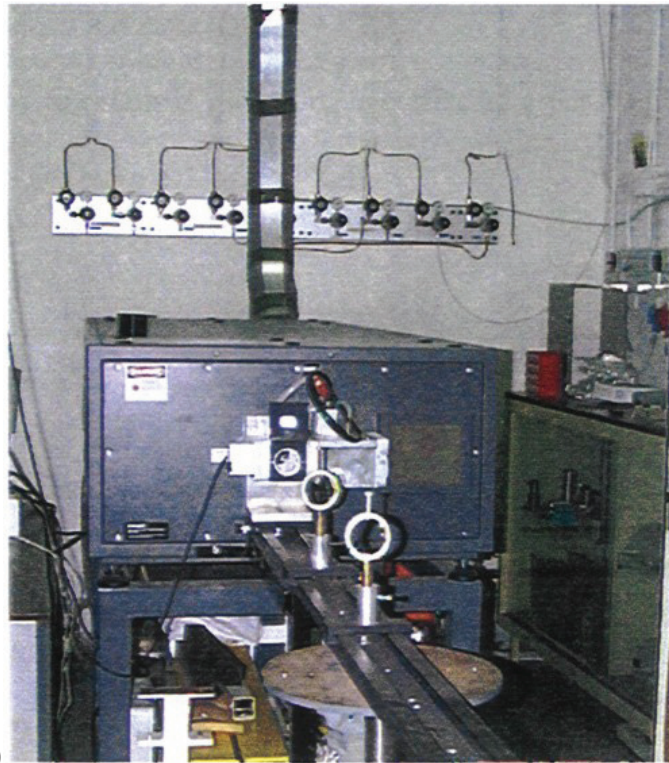
Characterization of airborne particulate matter has been a major challenge to researchers. Knowledge of the aerosol optical properties assumes significant importance in the wake of studies strongly correlating airborne particulate matter with adverse health effects. The small aerosol component, PM<sub>2.5</sub>, is of most concern to human health because it can be easily inhaled deep into the lungs. Along with health issues, aerosol particle distributions have significant implications for natural environment aesthetics and climatic change conditions. Increasing aerosol loading of

the atmosphere can lead either to an increase or decrease in the mean global temperature of Earth, depending on the optical properties. One of the main instrumentation that can be used for this investigation is lidar. A Raman lidar (Light Detection And Ranging) can be implemented in the straightforward fashion illustrated in Fig.1a. The system, whose principle scheme is described in Fig. 1b, operates by transmitting a laser pulse of arbitrary wavelength  $\lambda_0$  and recording radiation backscattered from the atmosphere as function of time to provide range information in a similar manner to a radar system. The return signal contains a strong elastically scattered component (at  $\lambda_0$ ) that is useful for profiling clouds and aerosols and also weaker inelastic scattered components that provide chemical-specific information. For profiling water vapor, we use components produced by vibrational Raman effect that produces energy shifts characteristic of the molecules in the atmosphere ( $3652\text{ cm}^{-1}$  for water vapor,  $2331\text{ cm}^{-1}$  for nitrogen).

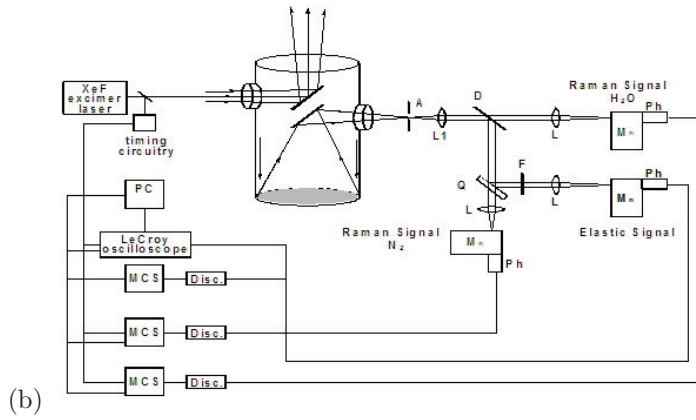
The aim of this paper is to process lidar backscattered signal that contains water vapor and aerosol information in order to improve their recovery; so it will be possible to find aerosol extinction for different filtering orders. Since they are affected by different kinds of noise, an appropriate filtering, with an improved recovery, represents a way to get good estimates of the above components.

The noise amount is overall but we describe in this work how to discriminate different types of noise; we concentrate our attention to the modeling of tedious noising coming from acoustic vibration in the telescope and heating scattering in the lidar apparatus. Noise coming from other sources, e.g. electrical and electronic systems can be easily faced.

The paper is organized in the following manner. Paragraph 1 deals with the theoretical aspects of water vapor calculations in order to get calibration signal. Paragraph 2 describes the experimental instrumentation. In § 3, we illustrate the techniques that allow us to recovery aerosol extinction by means of filtering and layer by layer integration; we present an alternate way to poissonian averaging with good results. Even if we have reached our purposes in distinguishing aerosol extinction from noise, this noise is an overall one so we indicate a manner of modeling it in different “sub noises”; that is what is faced in § 4. A summary and conclusions are outlined.



(a)



(b)

Fig. 1. Raman lidar. (a) The straightforward fashion. (b) Used lidar principle scheme.

## 2. Theoretical aspects

The water-vapor mixing ratio (grams of water per kilogram of dry air) as a function of range  $w(z)$  is proportional to the ratio of the number density of water vapor to nitrogen:

$$w(z) \simeq \frac{n_{wv}(z)}{n_{nit}(z)} \quad (1)$$

where  $n_{wv}(z)$  and  $n_{nit}(z)$  represent water vapor density and nitrogen one respectively. The nitrogen detection channel is always operated [1] with a filter that transmits the nitrogen Raman signal. The water-vapor channel, normally operated with a filter that transmits the water-vapor Raman signal, is also operated with a filter that transmits the nitrogen Raman signal. The direct ratio of the water-vapor and nitrogen channels operated with their normal filters and collecting various constants into  $k_{meas}$  yields to  $R_{meas}(z)$ , that is the calibration signal:

$$R_{meas}(z) = \frac{S_{wv,\lambda_{wv}}(z)}{S_{nit,\lambda_{nit}}(z)} \quad (2)$$

with  $S_{wv,\lambda_{wv}}(z)$  is the signal strength for water vapor while  $S_{nit,\lambda_{nit}}(z)$  is the signal strength for nitrogen and  $z$  the altitude. This ratio, which is close to goal represented in equation (1), is independent of laser power and attenuation of the laser beam propagating to the observation point and has the range-squared signal dependence removed [2]. Three ratio terms remain to be dealt with. The filter transmission functions  $T$  have little if any range dependence (created only by the change of the angle of the ray bundles passing through the filter with range), and any range dependence becomes negligible by forming the ratio of two channels with similar filters [3]; the term is generally only present in these equations for completeness. At various intervals during data acquisition, a nitrogen interference filter replaces the water-vapor filter in the water-vapor channel, and a measurement is recorded in this configuration. By use of equation (2) to calculate the ratio of the water-vapor channel and nitrogen channel signals, almost all the terms drop out because both channels are detecting nitrogen; the remaining terms form a calibration signal  $R_{cal}(z)$ :

$$R_{cal}(z) = \frac{S_{wv,\lambda_{wv}}(z)}{S_{nit,\lambda_{nit}}(z)} \quad (3)$$

$$= k_{cal} \frac{T_{wv,\lambda_{wv}}(z) O_{wv,\lambda_{wv}}(z)}{T_{nit,\lambda_{nit}}(z) O_{nit,\lambda_{nit}}(z)} \quad (4)$$

with  $T_{wv,\lambda_{wv}}(z)$ : filter transmission function for water vapor,  $T_{nit,\lambda_{nit}}(z)$ : filter transmission function for nitrogen and  $k_{cal}$ : calibration coefficient.

The ratio of the overlap terms  $O$  for the two channels can lead to a significant correction. Finally, taking the ratio of equations (2) and (4), we obtain:

$$\frac{R_{meas}(z)}{R_{cal}(z)} = \frac{k_{meas}}{k_{cal}} \frac{T_{wv,\lambda_{wv}}}{T_{wv,\lambda_{nit}}} \frac{O_{wv,\lambda_{wv}}}{O_{wv,\lambda_{nit}}} \frac{q}{q_{nit}} \frac{n}{n_{nit}} \quad (5)$$

with  $k_{meas}$ : constant present in lidar main equation,  $q$ : signal attenuation outgoing laser beam,  $q_{nit}$ : signal attenuation outgoing nitrogen channel,  $n$ : signal density,  $n_{nit}$ : nitrogen density. This result is similar to equation (2), but the ratio of the two overlap terms is now for a single channel (water vapor) although observed at two wavelengths, and would be strictly unity in a perfectly achromatic system. The overall ratio expressed in equation (5) should therefore be a better approximation to the goal represented in equation (1). In spite of optical filters included in the experimental apparatus, there is a need of further filtering, by using signal digital filtering. Equation (2) and equation (5) have been simplified in their specifications in order to make them easier in terms of meaning.

### 3. Experimental instrumentation

The lidar system (UNI-LE, 40°20'N, 18°6'E) operates in Physics Department of The University of Lecce (Italy). It uses an XeF excimer laser (lambda Physik LPX 210i) as illustrated in Fig.1a. An unstable cavity has been applied to the laser source to get a low divergence of laser beam. The laser, equipped with an unstable cavity, sends pulses of 150 mJ, with 30 ns of duration,  $30 \times 20 \text{ mm}^2$  of section and about 0.3 mRad of divergence. The collected backscattered radiation is obtained by a newtonian telescope whose primary mirror has 3 cm of diameter and 120 cm of focal length. The gathered radiation is spatially filtered by a diaphragm and separated in three different spectral channels corresponding to water vapor Raman radiation, to elastically scattered radiation and nitrogen scattered Raman radiation.

### 4. Method

Extinction is the total attenuation due to scattering and absorption of molecular and aerosol particles in the atmosphere. For the wavelengths selected, the extinction is predominantly from optical scattering due to

airborne particulate matter. A telescope form factor is used to aid in correcting and analyzing the surface level signals (up to an altitude of 800 *m*). The telescope form factor is introduced to correct the received signal vertical profile at low altitudes where the out-of-focus ray bundle overfills the detector, which is caused by the near field effect below 800 meters. The form factor used in this analysis is calculated from the return signal curves obtained under clear weather conditions. Water vapor signal filtering is the alternate way to determine extinction coefficient then aerosol extinction.

In the laser detection by means of lidar, there are five types of noise: *backscattering noise*, *quantum noise*, *statistical noise*, *dark current noise* and *noise due to optical elements*.

To discriminate noises [4] from the main signal that is backscattered from sky, we are investigating on the use of appropriate digital filtering to be utilized in order to retrieve a noiseless signal.

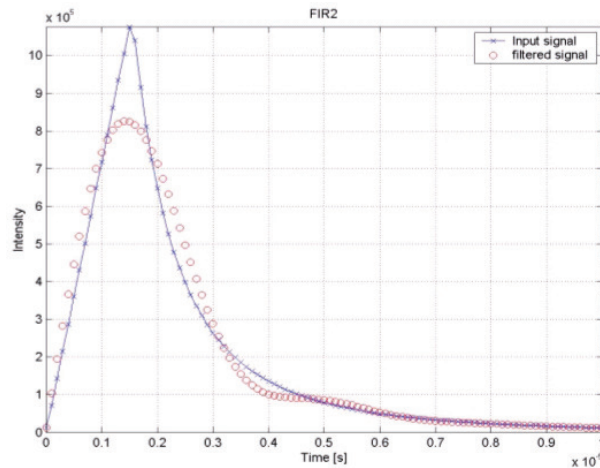


Fig. 2. Water vapor signal filtering.

This approach is different from the current one that uses a poissonian averaging of collected data. In the first level of our investigation, we prefer to employ filters that preserve either amplitude information and phase one. In this outlook, we have to use various filtering technique to improve data retrieval from back scattered signal [5]; that is, Finite-Impulse Response (FIR) or non-recursive filters, least-squares filters, adaptive filters and ARMA (Auto Regressive Moving Average), etc. We have chosen to use normal FIR (Fig.2) and least-squares filters so

that phase and amplitude information contained in the lidar signal must be preserved.

To design the filter, following steps have been performed:

- *Specifications for digital filter*: low-pass filter with sampling frequency  $f_s = 10 \text{ GHz}$ , cut off frequency  $f_c = 400 \text{ kHz}$  and pass band ripple of  $1 \text{ dB}$  or less as specified in Fig.3.

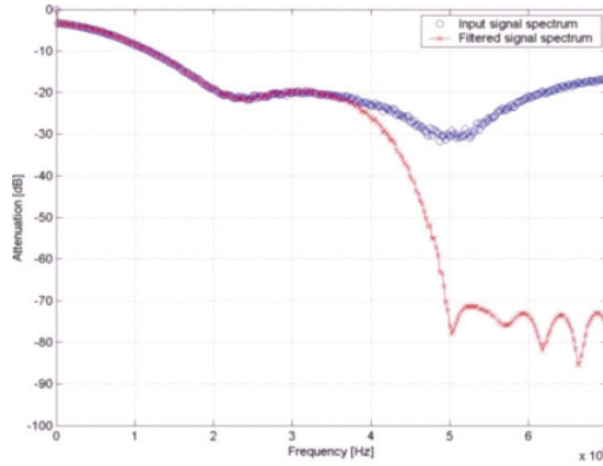


Fig. 3. Normal FIR filter outputs.

- *Approximation problem*: obtain an input-output characterization of the filter (such as transfer function) that satisfies the specifications;
- *Realization problem*: obtain a realization that defines the internal structure of filter that has transfer function  $H(z)$ . The realization is chosen to optimize criteria associated with the actual computation. The resulting vector of filtering must be put in the following equation in order to obtain aerosol extinction profile that is correlated to water vapor, that is:

$$\alpha^{aer} = \frac{\frac{d}{dz} \ln \left( \frac{z^2 s}{\rho} \right) - \alpha_{\lambda_L}^{ray}(z) \left( 1 - \left( \frac{\lambda_L}{\lambda_R} \right)^4 \right)}{1 + \left( \frac{\lambda_L}{\lambda_R} \right)^k} \quad (6)$$

where  $\alpha$  is extinction coefficient (aerosol and rayleigh ones),  $\rho$  stands for air density,  $z^2s$  is the filtered signal,  $\lambda_L$  and  $\lambda_R$  are respectively lidar wavelength and Raman one.

Quantitative measurements [6] of aerosol optical properties using a lidar system, which measures only aerosol backscatter, require accurate system calibration and assumptions regarding aerosol optical properties [7]. Lidar systems which scan can alleviate some of these restrictions by using a multi angle integral solution of the lidar equation to solve for both backscatter and extinction. However, this method requires horizontal homogeneity of the aerosol. We summarize the path followed to reach the aerosol extinction trend shown in Fig.4a:

- signal samples are acquired from the experimental apparatus described in section 2;
- a designed filtering system is utilized to discriminate actual and significant signal from noise, instead of producing signal from average poissonian-calculated sample vector;
- aerosol extinction is computed from equation (6) in two versions: numerically and functionally. The numerical way has a step trend. Extinction calculated according to numerical way becomes zero (Fig.4b) when altitude is 2500 meters.

Fig.5 indicates aerosol extinction trend with a real aperture. It shows the correct distribution in the space. That is a good value according to specific and scientific literature. For each experiment in with frequency around 400 kHz, we have found many different water vapor peaks that have processed in order to get a geometrical loci according to equation (6). The plot shows a correct trend due to a good filtering design.

In Fig.6 we see aerosol profile obtained with an error band. The band represents an oscillation of aerosol recovering because of different types of noise in the lidar system. An incorrect accomplishment of data acquisition and data analysis can determine a miscalculation in the estimation of the aerosol coefficient and of the statistical error. For this reason, huge care is necessary in handling data in order to retrieve the extinction coefficient profile starting from Raman signals [8].

The results reported in Fig.(4)a reflect the noctitime operations using the above XeF excimer laser; the outgoing wavelength is at 351 nm. In general, for 351 nm XeF excimer, the return Raman  $N^2$  wavelength is



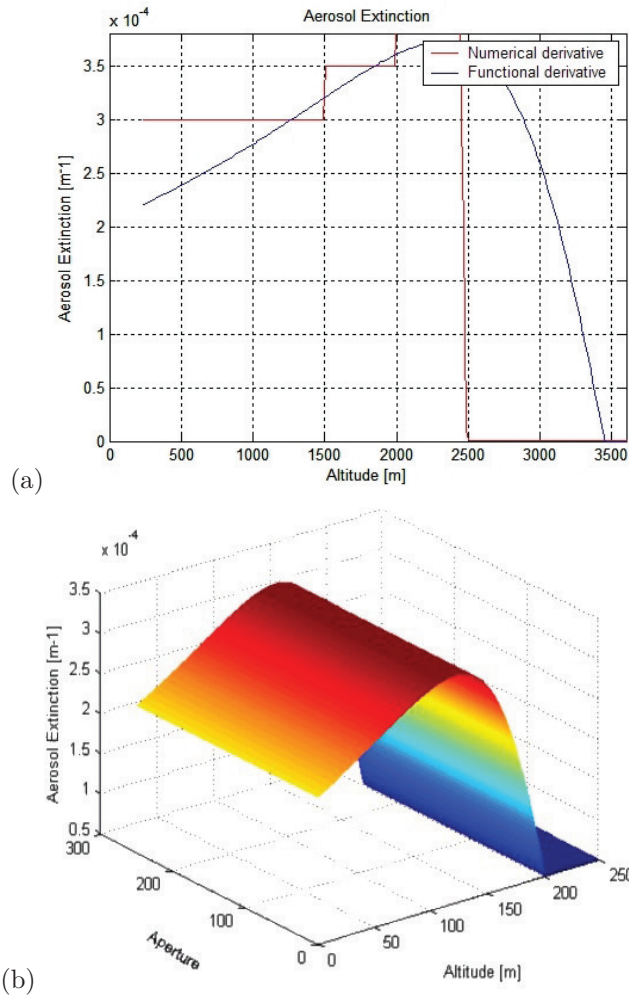


Fig. 4. (a) Aerosol extinction trend. (b) Spatial aerosol extinction trend.

at  $383 \text{ nm}$  and the return Raman  $O_2$  at  $372 \text{ nm}$ . Thus the total aerosol extinction measured by lidar is actually the sum of the aerosol extinction coefficients at  $351 \text{ nm}$  and at  $383 \text{ nm}$  if the Raman nitrogen signal is used or the sum of the aerosol extinction coefficients at  $351 \text{ nm}$  and  $372 \text{ nm}$  if the Raman oxygen signal is used.

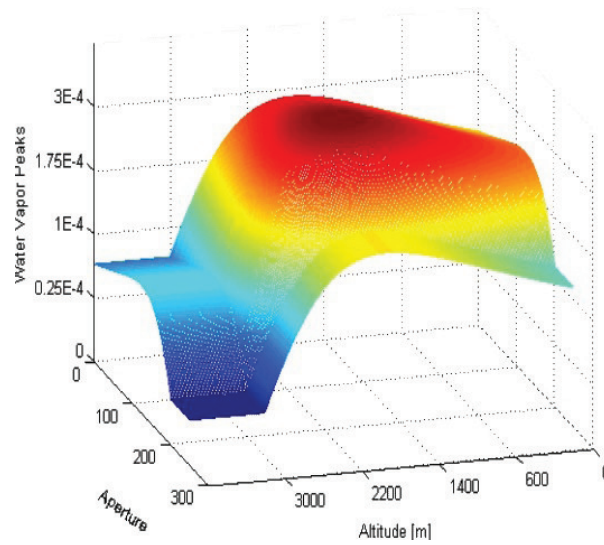


Fig. 5. Water vapor geometrical loci.

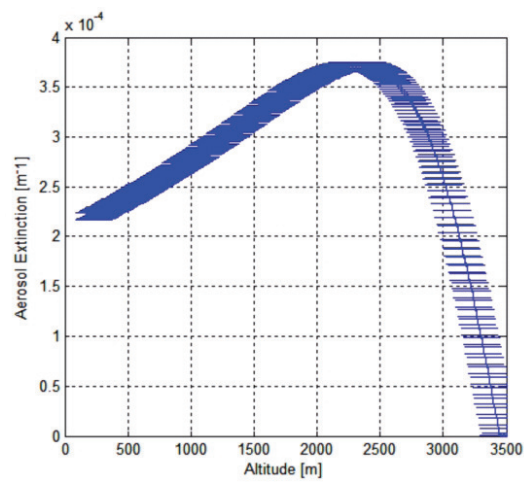


Fig. 6. Spatial-domain extinction with error band.

## 5. Noise modeling

The aim of this paragraph is to describe how it is possible to get a modeling of two main noise types: noise from temperature distribution in a metallic bar inside lidar and from acoustic vibration in the telescope.

**Heating noise**

We have to use Fourier series to model heating noise; since  $\int_{-\pi}^{+\pi} f(x) dx$  is absolutely convergent. In this case the Fourier series associated to  $f(x)$  is convergent, and its sum  $F(x)$  is equal to  $f(x)$  in any point of the range  $[-\pi, +\pi]$  in which  $f(x)$  is continue; it is equal to the arithmetic average of right limit and left one of  $f(x)$  in all points where  $f(x)$  has a first specie discontinuity:

$$F(\xi) = a_0 + \sum (a_n \cos n\xi + b_n \sin n\xi) = \frac{1}{2} \left\{ \lim_{x \rightarrow \xi^-} f(x) + \lim_{x \rightarrow \xi^+} f(x) \right\} \quad (7)$$

and for values of  $x$  external to the range  $[-\pi, +\pi]$ , it represents a function that repeats, with period  $2\pi$ , the trend of  $F(x)$  in the range  $[-\pi, +\pi]$ .

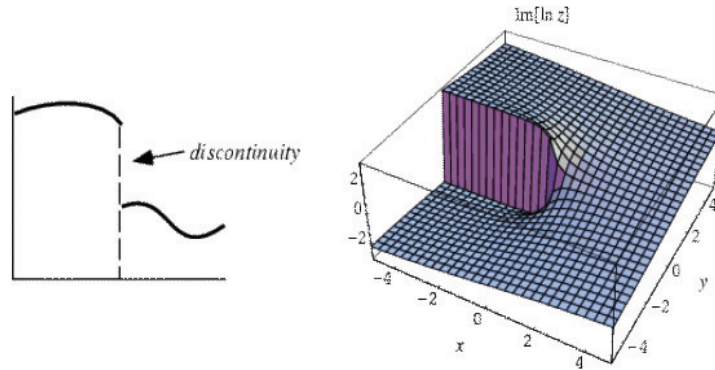


Fig. 7. Discontinuity.

Fig.7 describes discontinuity; in the right case, the discontinuity is a branch cut along the negative real of the natural logarithm  $\ln z$  for complex  $z$ . That is our case. Now we face the noise modeling due to heating scattering in lidar apparatus, especially in physical circuitry. Since we define relationship (7), we can declare:

$$\sigma(\omega) = \frac{1}{2\pi} \int_{-\infty}^{+\infty} \varphi(\xi) e^{-j\omega\xi} d\xi \quad (8)$$

where we use  $\xi$  in substitution of  $x$  as integration variable to avoid confusion,  $\varphi$  is the Fourier distribution of temperature and  $\sigma$  is a distribution to be determined, simplified from a general formulation of heat propagation problem in a bar we encounter in Physics. According to Fourier

properties:

$$\vartheta = \frac{1}{2} \int_{-\infty}^{+\infty} [\alpha(w)e^{jwx} + \bar{\alpha}(w)e^{-jwx}] e^{-w^2\Lambda t} d\omega \quad (9)$$

Where  $\Lambda$  is a positive amount,  $w^2$  is also positive and the term  $e^{-w^2\Lambda t}$  tends to zero when  $t$  goes to infinite for positive values, thus the solution maintains finite values. We can also write:

$$\vartheta = \frac{1}{4\pi} \int_{-\infty}^{+\infty} d\xi \int_{-\infty}^{+\infty} \varphi(\xi) [e^{jw(x-\xi)} + e^{-jw(x-\xi)}] e^{-w^2\Lambda t} d\omega \quad (10)$$

that is:

$$\vartheta = \frac{1}{2\pi} \int_{-\infty}^{+\infty} d\xi \int_{-\infty}^{+\infty} \varphi(\xi) \cos(w(x-\xi)) e^{-w^2\Lambda t} d\omega \quad (11)$$

Now we suppose, initially, heat was concentrated at point  $\xi = 0$ . That can be expressed with a function  $\delta$  (Dirac function) as following. Let are:  $Q$  the heat amount contained in a metallic connecting bar inside the lidar apparatus,  $\rho$  the density that is supposed constant,  $dV$  a volume element of the wire, the heat increment per time unit is:

$$Q = \int_{-\infty}^{+\infty} \rho\lambda\theta S dx \quad (12)$$

where  $S$  is the section of wire. Let us suppose  $\theta = \varphi$  that is initially null in any point, except in the origin where it is infinitely great; we can write:

$$\varphi = K\delta(x) \quad (13)$$

By substituting in previous equality, we see:

$$Q = \rho\lambda SK \int_{-\infty}^{+\infty} \delta(x) dx = \rho\lambda SK \quad (14)$$

that is enough to define  $K$ . We assume the last relationship representing a temperature distribution that can be inserted in equation (8) and integrated with respect to  $\xi$ , so we get:

$$\theta(x, t) = \frac{k}{2\pi} \int_{-\infty}^{+\infty} \cos(wx) e^{-w^2\Lambda t} d\omega \quad (15)$$

as an expression of temperature distribution in any instant  $t$ . We give it an acceptable form by setting  $w^2\Lambda t = \tau^2$ ,  $\nu = \frac{x}{\sqrt{\Lambda t}}$  and it results:

$$\theta = \frac{k}{2\pi\sqrt{\Lambda t}} \int_{-\infty}^{+\infty} e^{-\tau^2} \cos(\nu\tau) d\tau \quad (16)$$

By deriving with respect to  $\nu$  and integrating:

$$\frac{\partial \theta}{\partial \nu} = \frac{-k}{2\pi\sqrt{\Lambda t}} \int_{-\infty}^{+\infty} \tau e^{-\tau^2} \sin(\nu\tau) d\tau = -\frac{\nu}{2}\theta \quad (17)$$

that yields to:

$$\theta(\nu) = \theta(0)e^{-\frac{\nu^2}{4}} \quad (18)$$

but, in general, it is:

$$\theta(0) = \frac{k}{2\pi\sqrt{\Lambda t}} \int_{-\infty}^{+\infty} e^{-\tau^2} d\tau = \frac{k}{2\pi\sqrt{\Lambda t}} \quad (19)$$

By replacing this relationship in (11) and returning to previous variables, in conclusion:

$$\theta(x, t) = \frac{k}{2\pi\sqrt{\Lambda t}} e^{-\frac{x^2}{4\Lambda t}} \quad (20)$$

If we plot the graph representing  $\theta$  in function of  $x$  for time values which are constant (Fig.8), we see that, with increasing time, it leans to flatten, that is temperature distribution tends to become uniform and the area between the distribution and the  $x$  axis, represents the total heat contained in the connecting bar, as we can notice from equation (20). Knowing the temperature distribution in the bar, it is easy to compute the noise according to traditional formulation.

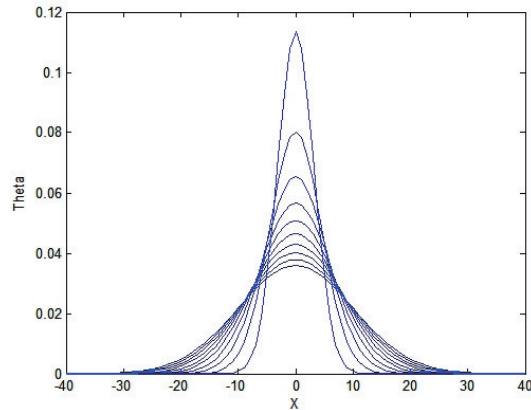


Fig. 8. Heat produced in lidar bar.

### Telescope noise

We know the beam generated by laser source reaches the mirror in the experimental lidar (Fig.9) after it has been reflected by a system of flat mirrors. The Newton-telescope (Fig.11), as declared in the beginning of this paper, collects backscattered radiation, and its primary mirror has 3 cm of diameter and 120 cm of focal length. The telescope is contained in a cylindrical aluminum case having length  $L = 2$  m and diameter  $D = 30$  cm. The beam, because of air presence in the telescope, generates acoustic vibrations that produce noise to be described according to the below modeling (Fig.10).

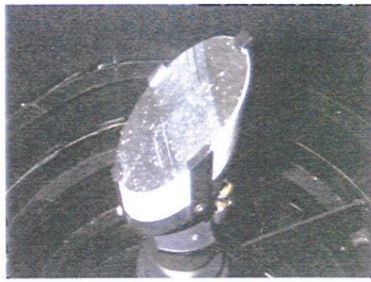


Fig. 9. Mirror view.

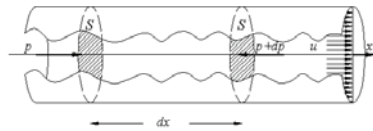


Fig. 10. Telescope modeling.

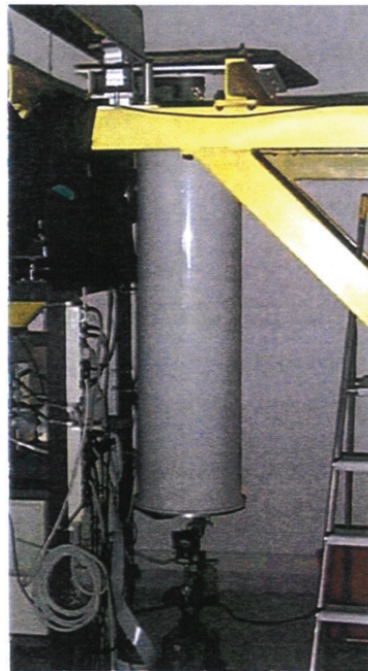


Fig. 11. Lidar newtonian telescope.

The modeling describes the air perturbation propagation in a cylindrical tube, supposing that perturbations are very small and constant. Let us, now, suppose that the motion takes place so that each air layer is normal to the tube axis and moves along the axis. If  $S$  is the tube

section,  $\rho$  is air density and  $p$  is pressure that acts on a layer:

$$p = A\rho^\gamma \quad (21)$$

where  $\gamma$  is the ratio between specific heat at constant pressure and specific heat at constant volume. Let us  $u$  the speed in a small amount and density variations also small. Setting  $\rho_0$  as air density in state of rest: consequently  $\rho = \rho_0(1 + s)$  with  $s \ll 1$ . We have to see air behavior included in two sections far  $dx$ . Air mass balance is:

$$\rho S dx = \rho_0(1 + s) S dx \quad (22)$$

the mass increment per time unit is:

$$\frac{\partial}{\partial \tau} (\rho S dx) = \rho_0 \frac{\partial s}{\partial t} S dx \quad (23)$$

and:

$$\begin{aligned} \left( \rho + \frac{\partial \rho}{\partial x} dx \right) S \left( u + \frac{\partial u}{\partial x} dx \right) &= \rho S u + \left( \rho S + \frac{\partial u}{\partial x} + S u \frac{\partial \rho}{\partial x} \right) dx \\ &= \rho S u + \left[ \rho_0(1 + s) S \frac{\partial u}{\partial x} + \rho_0 \frac{\partial S}{\partial x} S u \right] dx \\ \frac{\partial s}{\partial t} &= - \frac{\partial u}{\partial x} \end{aligned} \quad (24)$$

with  $u$ : the speed,  $S$ : the known section,  $s$ : the variable section using momentum definition and taking into account equation: (21)

$$-A\gamma\rho^{\gamma-1} \frac{\partial \rho}{\partial x} S dx = -A\gamma\rho_0^{\gamma-1} (1 + s)^{\gamma-1} \rho_0 \frac{\partial s}{\partial x} S dx = -A\gamma\rho_0^\gamma S \frac{\partial s}{\partial x} dx \quad (25)$$

since the current air momentum is:

$$u\rho S dx = u\rho_0 S dx \quad (26)$$

we get:

$$-a^2 \frac{\partial s}{\partial x} = \frac{\partial u}{\partial t} \quad (27)$$

where we set:

$$a^2 = A\gamma\rho_0^{\gamma-1} \quad (28)$$

by cancelling  $s$  in (22) and (27) we get an equation that determines  $u$ :

$$\frac{\partial^2 u}{\partial x^2} - \frac{1}{a^2} \frac{\partial^2 u}{\partial t^2} = 0 \quad (29)$$

Equation (22) describes the acoustic modelling that generates noise in the telescope.

## 6. Conclusion

In this paper we used digital filtering in order to retrieve lidar signal data by presence of water vapor. Water vapor and aerosols are two significant atmospheric components that are generally detected for a better knowledge of weather and climate. Aerosols play a key role in Earth's radiation balance and in the global climate, since they influence the radiation balance through two crucial processes: directly, by scattering and absorbing solar radiation, and indirectly, by acting as cloud condensation nuclei, and thus dramatically affecting the optical properties of clouds. The water vapor mixing ratio, on the other hand, is useful as a tracer of air parcel and in understanding energy transport mechanisms within the atmosphere.

The technical items faced in this paper are part of lidar network that allows to establish a climate data set of aerosol and water vapor vertical distributions in a quantitative and coordinated approach. The main objectives of the lidar network are to:

- perform lidar measurements of water vapor and aerosols on a fixed schedule to provide an unbiased statistically significant data set that allows to investigate the correlation between these two interesting atmospheric parameters besides providing quantification of their distribution and variability in space and time. Combined Rayleigh-Raman lidars based on a XeF excimer laser (351 nm) will be used in the network;
- perform additional measurements to specify important processes that are localized either in space or time such as those due to saharian dust outbreak, large forest fires and photochemical smog episodes. Continuous long-time lidar measurements will be carried out;
- provide ground truth for present and future satellite missions dedicated to the retrieval of the global water vapor and aerosols distribution. To this end the water vapor columnar content and the aerosol optical depth will be compared with satellite data.

It is believed that the data set provided as a result of the research activity performed within this network will be surely helpful for the scientific community, allowing a better modelling and a deeper understanding of the atmosphere physics. Despite the presence of interference filters inside the lidar instrumentation described in this paper, lidar signal output is affected by more noise. So far, in scientific literature, we



encountered the use of poissonian average, for each lidar acquisition, in order to retrieve water vapor; nevertheless, the approach provided by the present paper overcomes the above procedure and by using filtering [9], it is possible to remove noise, to get accurate acquisition and to have “one shot” (for further development) acquisition. Fig.12 summarizes, the objectives of this paper. In that figure, we see the illustration of signal variation in spatial-domain [10]. Although we have got aerosol extinction by filtering, we have promoted two models, from connecting bar and from newtonian telescope, that can help us to discriminate specific noise from the overall one. That leads us to the knowledge of each noise contribution.

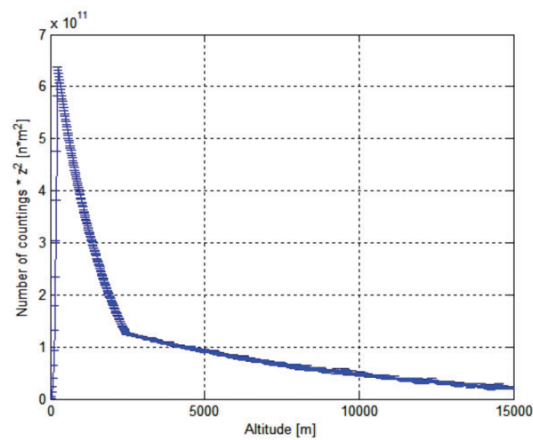


Fig. 12. Time-domain signal with error band.

## References

- [1] M.S. Unlu and S. Strite. Resonant cavity enhanced photonic devices. *J. Appl. Phys.*, 78(2):607-639, 1995.
- [2] J.E.M. Goldsmith, F.H. Blair, S.E. Bisson and D.D. Turner. Turn-key Raman lidar for profiling atmospheric water vapor, clouds and aerosols. *Applied Optics*, 37(21), July, 1998.
- [3] A. Ansmann, M. Riebesell, U. Wandinger, C. Weitkamp, E. Voss, W. Lahmann and W. Michaelis. Combined Raman elastic-backscatter lidar for vertical profiling of moisture, aerosol extinction, backscatter, and lidar ratio *Applied Physics*, B55, 18, 1992.
- [4] P.A. Lynn and W. Fuerst. *Digital signal processing with computer applications*. John Wiley & Sons, New York, 1993.

- [5] M. Belanger. *Digital processing of signals*. 2<sup>nd</sup> edition, Wiley, Chichester, 1989.
- [6] J.D. Klett. Stable analytical inversion solution for processing lidar returns. *Appl. Opt.*, 20: 211-220, 1981.
- [7] F.G. Fernald. Analysis of atmospheric lidar observations: Some components. *Appl. Opt.*, 23: 625-653, 1984.
- [8] D. Whiteman. Application of statistical methods to the determination of slope in lidar data. *Appl. Opt.*, 38(15):3360-3369, 1999.
- [9] R.W. Hamming. *Digital filters*. 2<sup>nd</sup> edition, Prentice-Hall, Englewood Cliffs, 1983.
- [10] S.D. Mayor , D. Shane, S.M. Spuler and B.M. Morley. NICAR'S New Raman-Shifted Eye-Safe Aerosol Lidar (REAL). 22<sup>nd</sup> *International Laser Radar Conference*, 12-16 July 2004, Matera, Italy.